Clinical and Molecular Epidemiological Features of Coronavirus HKU1–Associated Community-Acquired Pneumonia

Patrick C. Y. Woo,[1,a] Susanna K. P. Lau,[1,a] Hoi-wah Tsoi,[1] Yi Huang,[1] Rosana W. S. Poon,[1] Chung-ming Chu,[2] Rodney A. Lee,[3] Wei-kwang Luk,[4] Gilman K. M. Wong,[1] Beatrice H. L. Wong,[1] Vincent C. C. Cheng,[1] Bone S. F. Tang,[1] Alan K. L. Wu,[1] Raymond W. H. Yung,[3] Honglin Chen,[1] Yi Guan,[1] Kwok-hung Chan,[1] and Kwok-yung Yuen[1]

[1]Division of Infectious Disease, Department of Microbiology, The University of Hong Kong, [2]Division of Respiratory Medicine, Department of Medicine, United Christian Hospital, [3]Department of Microbiology, Pamela Youde Nethersole Eastern Hospital, and [4]Department of Pathology, Tseung Kwan O Hospital, Hong Kong, China

Background. Recently, we described the discovery of a novel group 2 coronavirus, coronavirus HKU1 (CoV-HKU1), from a patient with pneumonia. However, the clinical and molecular epidemiological features of CoV-HKU1–associated pneumonia are unknown.

Methods. Prospectively collected (during a 12-month period) nasopharyngeal aspirates (NPAs) from patients with community-acquired pneumonia from 4 hospitals were subjected to reverse-transcription polymerase chain reaction, for detection of CoV-HKU1. The epidemiological, clinical, and laboratory characteristics of patients with CoV-HKU1–associated pneumonia were analyzed. The *pol,* spike (S), and nucleocapsid (N) genes were also sequenced.

Results. NPAs from 10 (2.4%) of 418 patients with community-acquired pneumonia were found to be positive for CoV-HKU1. All 10 cases occurred in spring and winter. Nine of these patients were adults, and 4 had underlying diseases of the respiratory tract. In the 6 patients from whom serum samples were available, all had a 4-fold change in immunoglobulin (Ig) G titer and/or presence of IgM against CoV-HKU1. The 2 patients who died had significantl lower hemoglobin levels, monocyte counts, albumin levels, and oxygen saturation levels on admission and had more-extensive involvement visible on chest radiographs. Sequence analysis of the *pol,* S, and N genes revealed 2 genotypes of CoV-HKU1.

Conclusions. CoV-HKU1 accounts for 2.4% of community-acquired pneumonia, with 2 genotypes in the study population. Without performance of diagnostic tests, the illness was clinically indistinguishable from other community-acquired pneumonia illnesses.

Since no microbiological cause can be identifie in a significan proportion of patients with respiratory tract infections [1, 2], research has been conducted to iden-

tify novel agents. Of the 3 novel agents identifie in the last 3 years—including human metapneumovirus [3], severe acute respiratory syndrome (SARS) coronavirus (SARS-CoV) [4], and human coronavirus NL63 (HCoV-NL63) [5, 6]—2 are coronaviruses. On the basis of serological and phylogenetic characterization, coronaviruses were divided into 3 distinct groups: human coronavirus 229E (HCoV-229E) and HCoV-NL63 are group 1 coronaviruses, and human coronavirus OC43 (HCoV-OC43) is a group 2 coronavirus [7]. HCoV-229E and HCoV-OC43 account for 5%–30% of human respiratory tract infections [8], whereas, in a few recent studies, HCoV-NL63 was found to be present in 2%–3.6% of respiratory specimens [9–11]. In 2002 and 2003, the epidemic caused by SARS-CoV affected >8000 people, with 750 deaths [4, 12–18].

Table 1. Primers used for amplification and sequencing of the *pol*, spike (S), and nucleocapsid (N) genes.

Gene	Forward primer	Reverse primer
pol	LPW1465 5′-GTTCAAGTGTCGCTGTTCA-3′	LPW1822 5′-CTATCATTATCACAATCCACAG-3′
	LPW1467 5′-GGGTATGAAGTATCATCCTA-3′	LPW1825 5′-GATAATCCCAACCCATAAGAAC-3′
	LPW1826 5′-CATCTTATAAAGGATGTTGAC-3′	LPW1829 5′-ACAAACAACACATGCACCTACAC-3′
S	LPW1830 5′-TTGCCTATTATTTTACAAGGT-3′	LPW1864 5′-ACACTACCTATAACTATAGTAC-3′
	LPW1832 5′-TATGTTAATAAWACTTTGTATAGTG-3′	LPW1866 5′-TACAATTGACAAGAACTAGAAG-3′
	LPW1836 5′-GATTTGCARTTGGGCAGTTCTGG-3′	LPW1868 5′-CCATTAGAATCATACAAAAGAT-3′
	LPW1840 5′-GGTATTTTTAAAGAAGTTTCTGC-3′	LPW1870 5′-AGCTTCAACAAAACCWACATCTG-3′
	LPW1844 5′-TAGGTYCACAMTGYGGTTCTTC-3′	LPW1872 5′-AMCCTTGYTTAGGTGCAATACCT-3′
	LPW1848 5′-TTAAAACTGTYTTAGTAAGTCC-3′	LPW1874 5′-TAGTAAAACTAGTTAYAACACC-3′
N	LPW1887 5′-TAGTGGTATGGATACTGCCTTGT-3′	LPW1890 5′-GCTTTAACATTTCAGMATTACCA-3′
	LPW1891 5′-CAGTGTTTTGGTAAAAGAGGACC-3′	LPW1892 5′-TACCACCTAGTGTCGAATTAGG-3′

Recently, we have described the discovery of a novel group 2 coronavirus, coronavirus HKU1 (CoV-HKU1), from a patient with pneumonia [19]. Complete genome sequencing and phylogenetic analysis revealed that CoV-HKU1 is a distinct group 2 coronavirus, with G + C content of 32%, the lowest among all known coronaviruses. Although preliminary screening also identifie an additional patient with pneumonia with CoV-HKU1 in her nasopharyngeal aspirate (NPA), the epidemiological and clinical features of CoV-HKU1–associated pneumonia remain to be determined. In the present study, using prospectively collected NPAs, we examined the prevalence of CoV-HKU1 in patients with community-acquired pneumonia during a 12-month period. The clinical, laboratory, and radiological characteristics of patients with CoV-HKU1–associated

pneumonia were described. The molecular epidemiological profil of CoV-HKU1 was also analyzed.

PATIENTS AND METHODS

Patients and microbiological methods. All prospectively collected NPAs from patients with community-acquired pneumonia that were sent to the clinical microbiology laboratories of 4 hospitals in Hong Kong during a 12-month period (22 March 2003 [the beginning of the SARS epidemic in Hong Kong] to 21 March 2004) for detection of SARS-CoV and were found to be negative for SARS-CoV RNA, by reverse-transcription polymerase chain reaction (RT-PCR) [20], were included in the study. Community-acquired pneumonia is de-
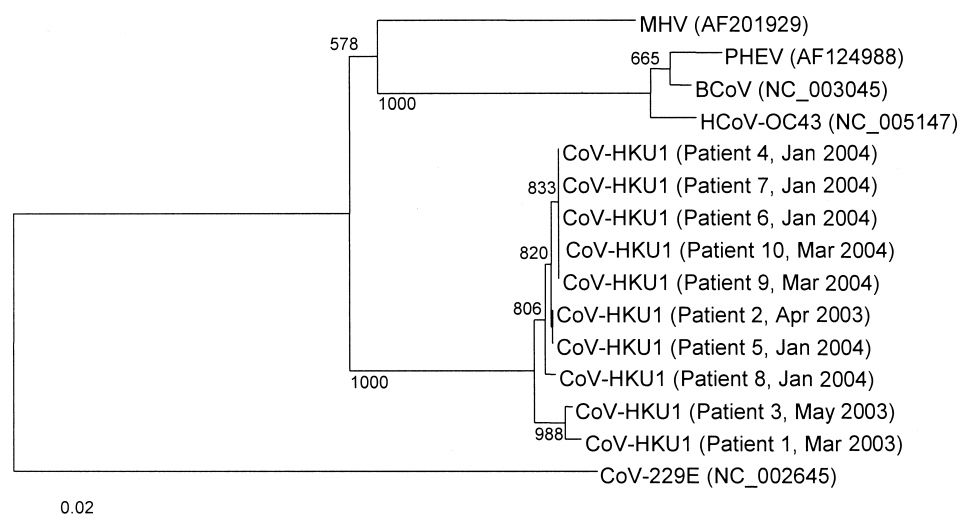

Figure 1. Phylogenetic tree of *pol* gene sequences of the 10 coronavirus HKU1 (CoV-HKU1) specimens from patients with community-acquired pneumonia. The tree was inferred from *pol* gene data by the neighbor-joining method, and bootstrap values were calculated from 1000 trees. The tree was rooted using the *pol* gene sequence of human coronavirus 229E (HCoV-229E), and 393 nt positions (primer sequences excluded) in each *pol* gene were included in the analysis. The scale bar indicates the estimated no. of substitutions per 50 bases using the Jukes-Cantor correction. BCoV, bovine coronavirus; HCoV-OC43, human coronavirus OC43; MHV, murine hepatitis virus; PHEV, porcine hemagglutinating encephalomyelitis virus.

Table 2. Epidemiological, clinical, and radiological characteristics of patients with community-acquired pneumonia associated with coronavirus HKU1.

Characteristic	1	2	3	4	5 [19]	6	7	8	9	10
Month/year	Mar/2003	Apr/2003	May/2003	Jan/2004	Jan/2004	Jan/2004	Jan/2004	Jan/2004	Mar/2004	Mar/2004
Sex/age, years	F/35	M/66	M/13	M/75	M/71	F/96	M/78	M/68	F/83	M/72
Ethnic origin	Chinese	Arabian	Chinese	Chinese	Chinese	Chinese	Chinese	Chinese	Chinese	Chinese
Underlying disease(s)	–	Diabetes mellitus, old myocardial infarction, gastric lymphoma	Asthma, situs inversus, dextrocardia	Hypertension	Chronic obstructive airway disease, hyperlipidemia, abdominal aortic aneurysm	Hypertension	Chronic obstructive airway disease, diabetes mellitus	–	Chronic obstructive airway disease, parathyroid adenoma, dementia	Prostate carcinoma, cerebrovascular accident, diabetes mellitus
History of travel within 2 weeks of disease onset	–	–	Shenzhen, China	Guangdong, China	Shenzhen, China	–	–	Guangdong, China	–	–
History of smoking	–	–	–	+	+	–	+	–	+	+
Clinical feature										
Fever	+	–	+	–	+	+	+	+	+	+
Chills	–	–	–	–	+	–	–	–	–	–
Rigor	–	–	–	–	–	–	–	–	–	–
Myalgia	–	–	–	–	–	–	–	–	–	–
Headache	–	–	–	–	+	–	–	–	–	–
Cough	+	–	+	+	+	–	+	+	–	+
Sputum production	–	–	+	+	+	–	+	+	–	+
Dyspnea	–	+	–	+	–	–	+	+	+	+
Pleurisy	–	–	–	–	–	–	–	–	–	–
Rhinorrhea	–	–	–	–	+	–	–	–	–	–
Sore throat	+	–	–	–	+	–	–	–	–	–
Oxygen saturation level on room air, %	99	83	100	99	99	97	97	95	99	88
Chest radiograph features	RLZ airspace shadows	Bilateral airspace shadows	LMZ and LLZ airspace shadows	LLZ airspace shadows	LLZ airspace shadows	RLZ airspace shadows	LLZ airspace shadows	RMZ airspace shadows	RLZ airspace shadows	Bilateral airspace shadows
Outcome	Survived	Died	Survived	Survived	Survived	Survived	Survived	Survived	Survived	Died
Duration of hospitalization, no. of days	2	Died on day 12	3	7	5	7	13	5	6	Died on day 6

NOTE. +, present; –, absent; LLZ, left lower zone; LMZ, left middle zone; LUZ, left upper zone; RLZ, right lower zone; RMZ, right middle zone; RUZ, right upper zone.

Table 3. Comparison of clinical, laboratory, and radiological characteristics of patients with coronavirus HKU1 (CoV-HKU1)–associated pneumonia and those of age- and sex-matched controls with non–CoV-HKU1–associated pneumonia.

| | Pneumonia[a] | | |
| | CoV-HKU1 | Non-CoV-HKU1 | |
Characteristic	(n = 10)	(n = 20)	P
Underlying diseases	8	12	.42
History of travel within 2 weeks of disease onset	4	6	.69
History of smoking	5	7	.46
Clinical features			
Fever	8	14	.68
Cough	7	17	.37
Sputum production	6	12	1.00
Dyspnea	6	6	.12
Rhinorrhea	1	2	1.00
Sore throat	2	2	.58
Hematological feature			
Hemoglobin concentration, g/dL	12.4	13.2	.27
Leukocyte count, $\times 10^9$ leukocytes/L	9.9	9.7	.95
Neutrophil count, $\times 10^9$ neutrophils/L	7.35	7.4	.71
Lymphocyte count, $\times 10^9$ lymphocytes/L	0.95	1.02	.48
Monocyte count, $\times 10^9$ monocytes/L	0.55	0.65	.35
Platelet count, $\times 10^9$ platelets/L	240	292	.20
Serum biochemical features			
Sodium concentration, mmol/L	136	137	.59
Potassium concentration, mmol/L	3.9	4.0	.42
Creatinine concentration, μmol/L	92	76.5	.06
Urea concentration, mmol/L	5.25	4.9	.62
Albumin concentration, g/L	37	38	.59
Globulin concentration, g/L	36.5	30	.07
Bilirubin concentration, μmol/L	12	10	1.00
ALT concentration, U/L	20	17	.42
Alkaline phosphatase concentration, U/L	102	91	.95
Oxygen saturation level on room air, %	96	98	.86
Radiological feature			
Bilateral involvement	2	5	1.00
No. of zones involved	1	1	.81
Mortality	2	0	.10

NOTE. ALT, alanine aminotransferase.

[a] Continuous variables are expressed as medians, and categorical variables are expressed as the no. of patients with the presence of the characteristic.

fine as symptoms and signs, consistent with an acute lower respiratory tract infection and associated with new radiographic findin for which there is no other explanation, that develop before or within 48 h after presentation to the hospital. Once CoV-HKU1 was detected in NPAs, hospital records, laboratory results (including direct antigen detection, by immunofluo escence, of influenz A and B viruses, parainfluenz viruses 1–3, respiratory syncytial virus [RSV], and adenovirus [21]), and chest radiographs of the corresponding patients were analyzed by 2 infectious-disease physicians. The RNA extracted from the NPAs was subjected to RT-PCR, for detection of influenz A virus and human metapneumovirus [4]. Available stored serum samples were subjected to serological assays, for detection of antibodies against *Mycoplasma*, *Chlamydia*, and *Legionella* spe-

cies and SARS-CoV, by SERODIA-MYCO II (Fujirebio), *Chlamydia pneumoniae* MIF IgG (Focus Technologies), indirect immunofluo escence (MRL), and our recently developed ELISA, respectively [16].

To determine possible risk factors associated with CoV-HKU1–associated pneumonia, 2 age- and sex-matched controls per patient with CoV-HKU1–associated pneumonia were randomly selected from patients with community-acquired pneumonia whose NPAs were found to be negative for CoV-HKU1. Controls were within 5 years in age (older or younger) of the corresponding patients with CoV-HKU1–associated pneumonia and were admitted within 15 days before or after admission of the corresponding patients with CoV-HKU1–associated pneumonia. The hospital records, laboratory results, and chest ra-
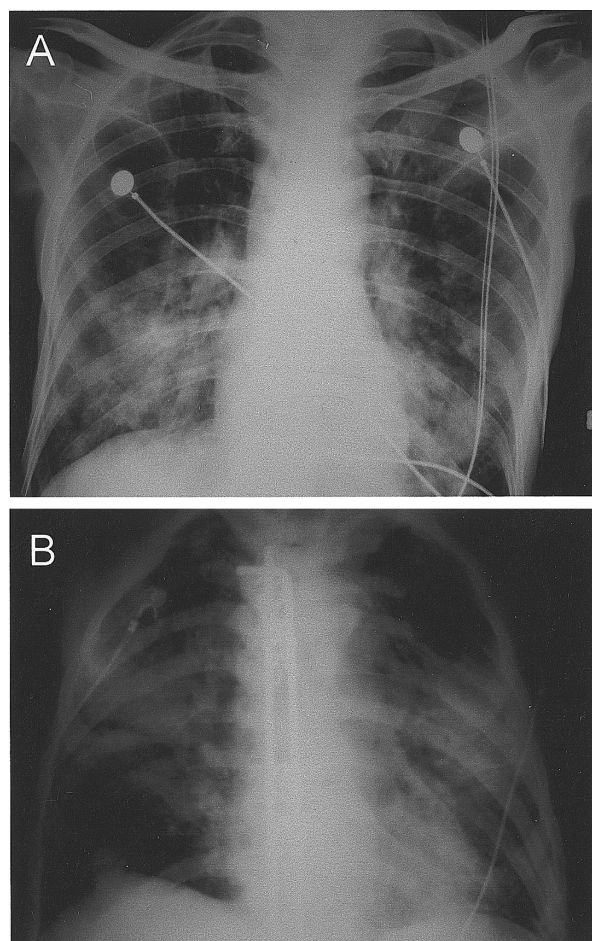
Figure 2. Chest radiographs of the 2 patients who died of coronavirus HKU1–associated community-acquired pneumonia. The chest radiograph of the first patient (*A*) (patient 2 in table 2) showed patchy airspace shadows in both lungs, with predominant involvement of the lower zones. The chest radiograph of the second patient (*B*) (patient 10 in table 2), with Luque instrumentation in situ, showed extensive airspace shadows in both lungs, with the middle zones more severely involved.

diographs of the controls were examined by 2 infectious disease physicians.

RNA extraction. Viral RNA was extracted from NPAs using the QIAamp Viral RNA Mini Kit (QIAgen) within 10 h of receipt of specimens. The eluted RNA (template for RT-PCR) was stored immediately at −70°C until use.

RT-PCR of the pol ***gene of CoV-HKU1 using CoV-HKU1–specifi primers and DNA sequencing.*** A 453-bp fragment of the *pol* gene of CoV-HKU1 was amplifie by RT-PCR using CoV-HKU1–specifi primers (LPW1926 [5′-AAAGGATGTTG-ACAACCCTGTT-3′] and LPW1927 [5′-ATCATCATACTAAA-ATGCTTACA-3′]) designed by multiple alignment of the nucleotide sequences of the *pol* genes of CoV-HKU1 [19] and those of other coronaviruses. RT was performed using the SuperScript II kit (Invitrogen). The PCR mixture (50 μL) contained cDNA, PCR buffer, 200 μmol/L each dNTP, and 1.0 U

of *Taq* polymerase (Boehringer). The mixtures were amplifie in 40 cycles of 94°C for 1 min, 48°C for 1 min, and 72°C for 1 min and a fina extension at 72°C for 10 min. To ensure the high specificit of the CoV-HKU1–specifi primers, RNA extracted from 200 NPAs positive for influenz A and B viruses, parainfluenz viruses 1–3, RSV, or adenovirus antigens and RNA from 12 NPAs positive for HCoV-229E, HCoV-OC43, HCoV-NL63, or SARS-CoV RNA (3 samples/coronavirus) were also subjected to RT-PCR using the 2 CoV-HKU1–specifi primers. The amplifie products were detected by agarose gel electrophoresis, as described elsewhere [19].

Both strands of the PCR products were sequenced twice by use of an ABI Prism 3700 DNA Analyzer (Applied Biosystems), using the 2 PCR primers. The sequences of the PCR products were compared with the sequences of the *pol* genes of CoV-HKU1 [19] and those of other coronaviruses in the GenBank database.

ELISA using recombinant nucleocapsid (N) protein of CoV-HKU1. The ELISA-based IgG and IgM antibody tests were performed in accordance with our published protocol [19]. Each sample was tested in duplicate, and the mean absorbance for each serum sample was calculated.

RT-PCR and sequencing of the complete pol, ***spike (S), and*** N ***genes of CoV-HKU1 and phylogenetic analysis.*** The complete *pol*, S, and N genes of CoV-HKU1 from NPAs from 9 of the 10 patients from whom adequate amounts of RNA were available were amplifie and sequenced using the strategy described in our previous study [19] and the primers listed in table 1. The nucleotide and deduced amino acid sequences of the *pol*, S, and N genes were compared with those of CoV-HKU1 [19] and other group 2 coronaviruses. Phylogenetic tree construction was performed using the PileUp method with GrowTree (Genetics Computer Group).

Statistical analysis. A comparison of characteristics was made between patients with CoV-HKU1–associated pneumonia and those with non–CoV-HKU1–associated pneumonia and between patients who died of and those who survived CoV-HKU1–associated pneumonia. Fisher's exact test was used for categorical variables, and the Mann-Whitney U test was used for continuous variables. $P < .05$ was regarded as statistically significant

RESULTS

Clinical and laboratory characteristics. During the 12-month period, NPAs from 418 patients (men:women, 198:220; mean ± SD age, 49 ± 26 years) in 4 hospitals with community-acquired pneumonia were found to be negative for SARS-CoV RNA by RT-PCR. A 453-bp fragment of the *pol* gene of CoV-HKU1 was amplifie and sequenced for 10 patients (2.4%). Sequence analysis revealed 0%–2% nucleotide differences between the sequences of the fragments and the sequence of the *pol* gene from

Table 4. Comparison of clinical, laboratory, and radiological characteristics of patients who survived and those who died of coronavirus HKU1–associated pneumonia.

| | Outcome[a] | | |
	Survived (n = 8)	Died (n = 2)	P
Characteristic			
Sex, M:F	5:3	2:0	1.00
Age, years	73	69	.60
Underlying diseases	6	2	.45
History of travel within 2 weeks of disease onset	4	0	.24
History of smoking	4	1	1.00
Clinical features			
Fever	7	1	.26
Cough	6	1	.51
Sputum production	5	1	.76
Dyspnea	4	2	.22
Rhinorrhea	1	0	.62
Sore throat	2	0	.45
Hematological feature			
Hemoglobin concentration, g/dL	13.4	9	.04[b]
Leukocyte count, $\times 10^9$ leukocytes/L	9.7	7.85	.43
Neutrophil count, $\times 10^9$ neutrophils/L	7.4	6.9	.79
Lymphocyte count, $\times 10^9$ lymphocytes/L	1.35	0.55	.15
Monocyte count, $\times 10^9$ monocytes/L	0.7	0.3	.04[b]
Platelet count, $\times 10^9$ platelets/L	292	200.5	.79
Serum biochemical feature			
Sodium concentration, mmol/L	137.5	134	.11
Potassium concentration, mmol/L	3.9	4.5	.06
Creatinine concentration, μmol/L	79	76.5	.69
Urea concentration, mmol/L	4.6	10.75	.19
Albumin concentration, g/L	38.5	26	.04[b]
Globulin concentration, g/L	30	30	1.00
Bilirubin concentration, μmol/L	10	30.5	.79
ALT concentration, U/L	16.5	30.5	.36
Alkaline phosphatase concentration, U/L	86	190.5	.07
Oxygen saturation level on room air, %	99	85.5	.03[b]
Radiological feature			
Bilateral involvement	0	2	.003[b]
No. of zones involved	1	6	.01[b]

NOTE. ALT, alanine aminotransferase.

[a] Continuous variables are expressed as medians, and categorical variables are expressed as the no. of patients with the presence of the characteristic.

[b] Difference is statistically significant.

the CoV-HKU1 in the NPAs from the reported index patient (patient 5) [19] (figure 1). In contrast, by use of our CoV-HKU1–specific primers, none of the 200 NPAs positive for influenza A and B viruses, parainfluenza viruses 1–3, RSV, or adenovirus antigens and none of the 12 NPAs positive for HCoV-229E, HCoV-OC43, HCoV-NL63, and SARS-CoV RNA were RT-PCR positive.

The epidemiological, clinical, and radiological characteristics of the 10 patients with CoV-HKU1–associated community-acquired pneumonia are summarized in table 2. No epidemiological linkage was identified among the 10 cases. All cases occurred during either spring or winter (January–May). The median age of these patients was 71.5 years (range, 13–96 years).

Seven were men, and 3 were women. Eight had underlying diseases, of whom 4 had underlying diseases of the respiratory tract. Four had recently traveled to southern China. Five were smokers. Clinically, the illness was not distinguishable from other community-acquired pneumonia illnesses. Fever, productive cough, and dyspnea were common symptoms at presentation. Upper respiratory tract symptoms were present in only 2 patients (patients 1 and 5). One patient (patient 7) had loose-stool diarrhea. Oxygen saturation levels on room air on admission were <95% in 2 patients. Airspace shadows were observed in the right lungs of 6 patients and in the left lungs of 6 patients. The upper, middle, and lower zones were affected in 2, 4, and 9 patients, respectively. All patients, except patient
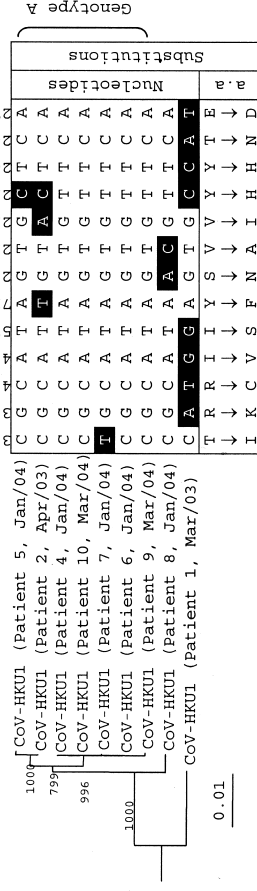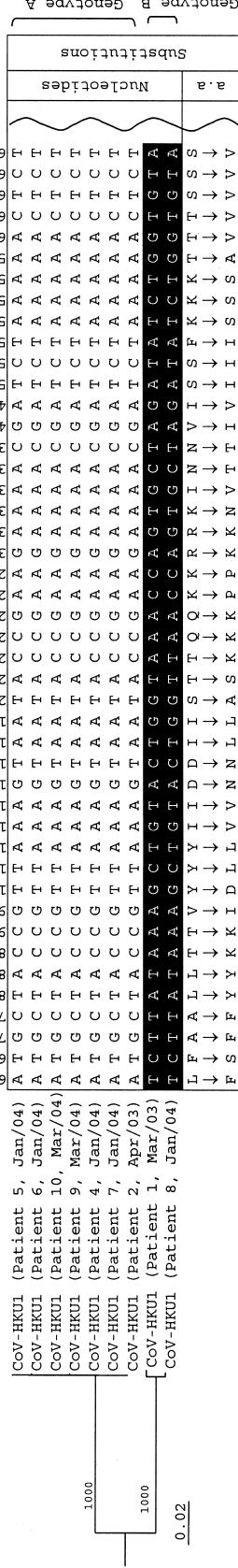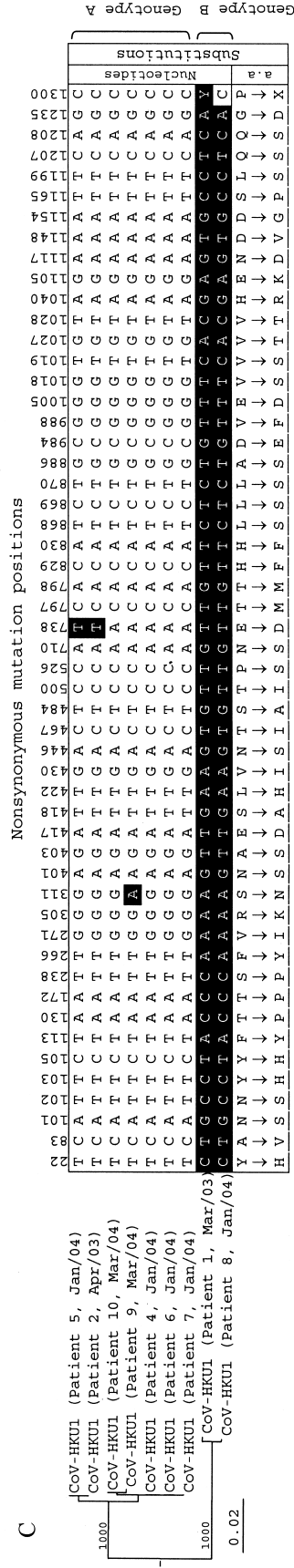
Figure 3. Phylogenetic trees and nonsynonymous mutations and corresponding amino acid changes of complete *pol*, spike (S), and nucleocapsid (N) gene sequences of coronavirus HKU1 (CoV-HKU1) specimens from 9 patients with community-acquired pneumonia. The trees were inferred from *pol* (3A), S (3B), and N (3C) gene data by the neighbor-joining method, and bootstrap values were calculated from 1000 trees. The trees were rooted using *pol*, S, and N gene sequences of human coronavirus OC43 (HCoV-OC43). A total of 2784 nt positions in each *pol* gene, 4071 nt positions in each S gene, and 1326 nt positions in each N gene were included in the analysis. The scale bar indicates the estimated no. of substitutions per 100 (*A*) and 50 (*B* and *C*) bases, using the Jukes-Cantor correction. The shaded nucleotides are those that differ from the majority at the corresponding location. Because of the large no. of nonsynonymous mutations in the S gene, only the NH₂ terminal 45, of a total of 306 nonsynonymous mutations, is shown.
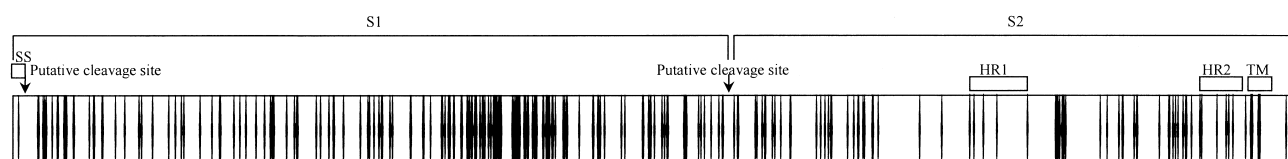
Figure 4. Distribution of nonsynonymous mutations in the spike (S) gene of coronavirus HKU1 (CoV-HKU1). The S protein (1356 aa) of CoV-HKU1 is depicted by the horizontal bar, and the positions of the nonsynonymous mutations are depicted by vertical lines in the bar. HR1, heptad repeat 1 (aa 982–1083); HR2, heptad repeat 2 (aa 1250–1297); SS, N terminal signal sequence (aa 1–13); TM, transmembrane domain (aa 1301–1323).

10, had normal platelet counts and normal results of liver and renal function tests. Bacterial or mycobacterial pathogens were not detected in any of the sputum samples from the patients. Results of direct antigen testing for influenza A and B viruses, parainfluenza viruses 1–3, RSV, and adenovirus and of RT-PCR for influenza A virus and metapneumovirus were negative for all NPAs. Results of testing for antibodies against *Mycoplasma pneumoniae, C. pneumoniae, Chlamydia psittaci, Legionella pneumophila,* and SARS-CoV were negative for all 6 patients (patients 1, 4, 5, 6, 8, and 9) from whom serum samples were available. Of these 6 patients, all had a 4-fold increase in IgG titer (patients 4, 5, and 6) and/or the presence of IgM against CoV-HKU1 (patients 1, 5, 8, and 9). Compared with age- and sex-matched controls with non–CoV-HKU1–associated pneumonia, patients with CoV-HKU1–associated pneumonia had no epidemiological, clinical, hematological, serum biochemical, or radiological risk factors identified (table 3). None of the 10 patients in this control group from whom serum samples were available had a 4-fold increase in IgG titer or the presence of IgM against CoV-HKU1.

Two of the 10 patients died of CoV-HKU1–associated pneumonia. The first patient (patient 2) was a 66-year-old man who had presented with dyspnea for 1 day. He had type 2 diabetes mellitus, old myocardial infarction, and gastric lymphoma with total gastrectomy in 2002 and was treated with chemotherapy. He had severe lymphopenia (0.2×10^9 lymphocytes/L) and an oxygen saturation level of only 83% on admission. Chest radiographic examination revealed patchy airspace shadows in both lungs, with predominant involvement of the lower zones (figure 2*A*). He died 11 days after admission. The other patient (patient 10) was a 72-year-old man who had presented with fever and productive cough for 1 week. He had type 2 diabetes mellitus, cerebrovascular accident, and prostatic carcinoma with bone metastasis complicated by spinal cord compression; laminectomy and Luque instrumentation were performed. He had lymphopenia (0.9×10^9 lymphocytes/L), thrombocytopenia (33×10^9 thrombocytes/L), deranged liver and renal function test results, and an oxygen saturation level of only 88% on admission. Chest radiographic examination revealed extensive airspace shadows in both lungs, with the middle zones more severely involved (figure 2*B*). He died 5 days after admission.

The clinical, laboratory, and radiological characteristics of patients who survived and those who died of CoV-HKU1–associated community-acquired pneumonia were compared (table 4). Patients who died had lower hemoglobin concentrations ($P = .04$), monocyte counts ($P = .04$), serum albumin levels ($P = .04$), and oxygen saturation levels on admission ($P = .03$) and had bilateral involvement ($P = .003$) and more zones involved ($P = .01$) on chest radiographs.

RT-PCR and sequencing of the complete* pol, *S, and N genes of CoV-HKU1 and phylogenetic analysis. The complete *pol*, S, and N genes of CoV-HKU1 from NPAs from 9 of the 10 patients from whom adequate amounts of RNA were available were amplified and sequenced. The phylogenetic trees and nonsynonymous mutations and the corresponding amino acid changes are shown in figure 3. For the S gene, there were 317 and 306 nt positions with synonymous and nonsynonymous mutations, respectively (figure 3*B*); 72% and 28% of the nonsynonymous mutations were in the putative S1 and S2, respectively (figure 4). For the N gene, there were 42 and 53 nt positions with synonymous and nonsynonymous mutations, respectively (figure 3*C*). The nucleotide sequences of 7 of the 9 S or N genes showed similar sequences (genotype A), and those of the other 2 genes also showed similar sequences (genotype B) (figure 3*B* and 3*C*). For the CoV-HKU1 specimen from patient 1, 2 peaks (T and C) were consistently observed at nt 1300 of the N gene, suggesting the presence of a quasi species (figure 3*C*). For the *pol* gene, there were 95 and 13 nt positions with synonymous and nonsynonymous mutations, respectively (figure 3A). The nucleotide sequences of the *pol* genes in the 7 CoV-HKU1 specimens of genotype A were also clustered together (figure 3*A*). Interestingly, the 7 CoV-HKU1 specimens of genotype A were from 7 patients with underlying diseases, and the 2 specimens of genotype B were from the 2 patients without underlying diseases (table 2). Furthermore, multiple alignments of the nucleotide sequences of the *pol* genes from the 9 CoV-HKU1 specimens and those from the HCoV-OC43, HCoV-229E, HCoV-NL63, and SARS-CoV supported the notion that the primers used in the present study were specific for CoV-HKU1.

DISCUSSION

CoV-HKU1, a novel group 2 coronavirus, is associated with community-acquired pneumonia. Since the SARS epidemic in 2003, we have started to prospectively collect NPAs from patients with community-acquired pneumonia and store the extracted RNA, so that, when a novel virus is discovered, the epidemiological and, hence, the clinical, laboratory, and radiological features of the disease can be studied in a timely manner. In January 2004, we discovered a novel coronavirus, CoV-HKU1, from a patient with community-acquired pneumonia [19]. The RNA extracted from prospectively collected NPAs was immediately retrieved, and the presence of CoV-HKU1 was investigated. Ten of the 418 NPAs were positive for CoV-HKU1, giving an incidence of 2.4%. The presence of CoV-HKU1 in these specimens was genuine—that is, it was not due to contamination—since amplification and sequencing of multiple genes (pol, S, and N) of CoV-HKU1 indicated the presence of CoV-HKU1 with different nucleotide sequences from the different patients. Moreover, the clinical significance of CoV-HKU1 was confirmed by the presence of a specific antibody response in all 6 patients from whom serum samples were available. The antibody response in these patients was unlikely to be the result of cross-reaction with other known human coronaviruses, since none of the 20 serum samples obtained from patients with HCoV-OC43 infections or SARS-CoV pneumonia had positive results in the recombinant N ELISA (authors' unpublished data). Further studies on detection of CoV-HKU1 in NPAs from healthy individuals will determine whether asymptomatic shedding of CoV-HKU1 occurs.

Similar to HCoV-229E, HCoV-OC43, and HCoV-NL63, CoV-HKU1 is a human coronavirus that is endemic in humans. Similar to other human coronavirus infections, cases of CoV-HKU1–associated pneumonia occurred during winter and spring. Most patients with CoV-HKU1–associated pneumonia were old (80% were >65 years old) and had major underlying diseases, especially those of the respiratory and cardiovascular systems. To study the phylogeny and relationships among the 10 CoV-HKU1 specimens, we sequenced the pol, S, and N genes from the 9 CoV-HKU1 specimens that contained adequate amounts of RNA. Combined with the data on partial sequencing of the pol genes from the 10 CoV-HKU1 specimens (figure 1), results showed that, unlike the epidemiological profile of SARS-CoV, the 10 CoV-HKU1 specimens were not clonal, and the topology of the phylogenetic trees did not follow the pattern of a clonal outbreak (figure 3). Interestingly, the phylogenetic trees constructed using the sequences of both the S and N genes showed that CoV-HKU1 of genotype B was detected in NPAs from with 2 patients without underlying diseases, but CoV-HKU1 of genotype A was detected in NPAs from patients with underlying diseases (figure 3B and 3C). Sequencing of more

CoV-HKU1 specimens may reveal the presence of genotypes or clades of CoV-HKU1 with differential virulence.

Compared with SARS-CoV pneumonia, CoV-HKU1–associated pneumonia is a monophasic disease, and most patients had relatively mild symptoms that were localized to the respiratory tract and were, therefore, hospitalized only briefly. SARS-CoV pneumonia is often described as a biphasic disease, with the first phase due to cell lysis as a result of viral replication and the second phase due to immunopathological damage [4, 12]. On the other hand, all 10 patients with CoV-HKU1–associated pneumonia showed the pattern of a monophasic disease. Although dyspnea was present in one-half of the patients with CoV-HKU1–associated pneumonia at presentation, compared with only ~20% of patients with SARS-CoV pneumonia at presentation [4], patients with CoV-HKU1–associated pneumonia often recovered quickly, but patients with SARS-CoV pneumonia deteriorated after 7–10 days [4, 12]. For the 8 patients who recovered, the median duration of hospitalization was only 5.5 days. This rapid recovery of patients with CoV-HKU1–associated pneumonia could be related to the rapid control of the virus by the immune system. This is in line with the results of our previous study, which showed that the index patient with CoV-HKU1–associated pneumonia had his peak viral load at around day 3 after the onset of illness [19]. Moreover, only 1 of the patients had extrapulmonary symptoms, and all available extrapulmonary specimens (stool, urine, and serum) were negative, by RT-PCR, for CoV-HKU1 (authors' unpublished data). On the other hand, for SARS-CoV pneumonia, patients usually had their peak viral loads 7–10 days after onset of illness [12]. Furthermore, the virus can be readily detected in extrapulmonary specimens, in which the viral loads correlated with the manifestations in the corresponding systems [22]. These findings imply that the virus was not well controlled by the immune system during the initial phase of the illness.

Despite the relatively mild course of disease in most patients, CoV-HKU1–associated pneumonia is associated with mortality in a minority of patients who have lower hemoglobin concentrations, monocyte counts, serum albumin levels, and oxygen saturation levels on admission and more-extensive involvement on chest radiographs. As in most cases of pneumonia, extensive involvement in the lungs will result in poor gaseous exchange and, hence, hypoxia and eventually death. The lower hemoglobin concentrations, monocyte counts, and serum albumin levels could represent poorer premorbid states and narrower margins to fight against infections. Both patients who died had underlying diabetes mellitus, malignancy (gastric lymphoma in one and prostate carcinoma in the other), and cardiovascular disease (old myocardial infarction in one and cerebrovascular accident in the other).

References

1. Macfarlane JT, Colville A, Guion A, et al. Prospective study of aetiology and outcome of adult lower-respiratory-tract infections in the community. Lancet **1993**; 341:511–4.
2. Ruiz M, Ewig S, Marcos MA, et al. Etiology of community-acquired pneumonia: impact of age, comorbidity, and severity. Am J Respir Crit Care Med **1999**; 160:397–405.
3. Van den Hoogen BG, de Jong JC, Groen J, et al. A newly discovered human pneumovirus isolated from young children with respiratory tract disease. Nat Med **2001**; 7:719–24.
4. Peiris JSM, Lai ST, Poon LLM, et al. Coronavirus as a possible cause of severe acute respiratory syndrome. Lancet **2003**; 361:1319–25.
5. van der Hoek L, Pyrc K, Jebbink MF, et al. Identificatio of a new human coronavirus. Nat Med **2004**; 10:368–73.
6. Fouchier RA, Hartwig NG, Bestebroer TM, et al. A previously undescribed coronavirus associated with respiratory disease in humans. Proc Natl Acad Sci USA **2004**; 101:6212–6.
7. Lai MM, Cavanagh D. The molecular biology of coronaviruses. Adv Virus Res **1997**; 48:1–100.
8. McIntosh K, Kapikian AZ, Turner HC, Hartley JW, Parrott RH, Chanock RM. Seroepidemiologic studies of coronavirus infection in adults and children. Am J Epidemiol **1970**; 91:585–92.
9. Bastien N, Anderson K, Hart L, et al. Human coronavirus NL63 infection in Canada. J Infect Dis **2005**; 191:503–6.
10. Arden KE, Nissen MD, Sloots TP, MacKay IM. New human coronavirus, HCoV-NL63, associated with severe lower respiratory tract disease in Australia. J Med Virol **2005**; 75:455–62.
11. Ebihara T, Endo R, Ma X, Ishiguro N, Kikuta H. Detection of human coronavirus NL63 in young children with bronchiolitis. J Med Virol **2005**; 75:463–5.
12. Peiris JSM, Chu CM, Cheng VCC, et al. Clinical progression and viral load in a community outbreak of coronavirus-associated SARS pneumonia: a prospective study. Lancet **2003**; 361:1767–72.
13. Zhong NS, Zheng BJ, Li YM, et al. Epidemiology and cause of severe acute respiratory syndrome (SARS) in Guangdong, People's Republic of China, in February. Lancet **2003**; 362:1353–8.
14. Guan Y, Peiris JSM, Zheng B, et al. Molecular epidemiology of the novel coronavirus causes severe acute respiratory syndrome. Lancet **2004**; 363:99–104.
15. Nicholls JM, Poon LL, Lee KC, et al. Lung pathology of fatal severe acute respiratory syndrome. Lancet **2003**; 361:1773–8.
16. Woo PCY, Lau SKP, Tsoi HW, et al. Relative rates of non-pneumonic SARS coronavirus infection and SARS coronavirus pneumonia. Lancet **2004**; 363:841–5.
17. Guan Y, Zheng BJ, He YQ, et al. Isolation and characterization of viruses related to the SARS coronavirus from animals in southern China. Science **2003**; 302:276–8.
18. Cheng VCC, Hung IFN, Tang BSF, et al. Viral replication in the nasopharynx is associated with diarrhea in patients with severe acute respiratory syndrome. Clin Infect Dis **2004**; 38:467–75.
19. Woo PCY, Lau SKP, Chu CM, et al. Characterization and complete genome sequence of a novel coronavirus, coronavirus HKU1, from patients with pneumonia J Virol **2005**; 79:884–95.
20. Yam WC, Chan KH, Poon LLM, et al. Evaluation of reverse transcription-PCR assays for rapid diagnosis of severe acute respiratory syndrome associated with a novel coronavirus. J Clin Microbiol **2003**; 41:4521–4.
21. Woo PCY, Chiu SSS, Seto WH, Peiris M. Cost-effectiveness of rapid diagnosis of viral respiratory tract infections in pediatric patients. J Clin Microbiol **1997**; 35:1579–81.
22. Hung IFN, Cheng VCC, Wu AKL, et al. Viral loads in clinical specimens and SARS manifestations. Emerg Infect Dis **2004**; 10:1550–7.